

# Comprehensive Correction of Artifacts due to Eddy Current-Induced Echo Shifts in Partial Fourier DTI

T-K. Truong<sup>1</sup>, N-K. Chen<sup>1</sup>, and A. W. Song<sup>1</sup>

<sup>1</sup>Brain Imaging and Analysis Center, Duke University, Durham, NC, United States

## Introduction

Partial Fourier (PF) echo-planar imaging (EPI) is typically used in diffusion tensor imaging (DTI) to reduce the TE and increase the signal-to-noise ratio (SNR). However, eddy currents induced by the diffusion gradients shift the echo from the center of k-space. Echo shifts along the phase-encoding direction  $\Delta k_y$  in turn lead to: (i) signal loss if the echo is shifted outside the acquired k-space (Fig. 1A, green area) (type 1 artifact), (ii) PF reconstruction errors if the echo is shifted outside the central k-space band from which the background phase is computed (Fig. 1C, yellow area) (type 2 artifact), and (iii) an increase or decrease of the effective TE, so that the acquired echo is an asymmetric spin-echo with an additional  $T_2^*$ -weighting rather than a pure spin-echo (Fig. 1E) (type 3 artifact).

All three types of artifact vary with spatial location and diffusion direction, leading to errors in the derivation of the diffusion tensor and consequently in fractional anisotropy (FA) maps and in fiber tractography. To avoid such artifacts, a large number of overscans (i.e., number of  $k_y$  lines acquired before the  $k_y = 0$  line) is required, thereby greatly limiting the benefits of PF imaging. Here, we propose a novel PF-DTI acquisition and post-processing method that can correct for all three types of artifact while maintaining a small number of overscans and hence a high SNR.

## Methods

To correct for type 1 artifacts, a gradient blip is added to the first phase-encoding gradient of the EPI readout (Fig. 1B, blue gradient) to adjust the acquisition window such that the shifted echo remains within the acquired k-space (green area). The appropriate blip depends on  $\Delta k_y$  and therefore varies with the diffusion direction and slice number. To measure  $\Delta k_y$  and determine the blips, we use k-space energy spectrum analysis (KESA) (1), which can inherently measure the eddy current-induced echo shifts from the DTI k-space data. Since the eddy currents are subject-independent, this calibration only needs to be performed once on a spherical gel phantom using the same parameters as the DTI scan.

To correct for type 2 artifacts, a multischeme PF reconstruction method (2) is used, in which the background phase is computed in a k-space band centered on the shifted echo (Fig. 1D, yellow area) rather than on the  $k_y = 0$  line. This procedure is repeated for all possible  $\Delta k_y$  values to generate a series of PF images. Depending on the magnitude of  $\Delta k_y$ , the missing data can be generated on the other side of k-space (arrow). The final image is formed by extracting each pixel from the appropriate PF image according to its  $\Delta k_y$  value, which is obtained from a  $\Delta k_y$  map computed with KESA from the DTI data.

To correct for type 3 artifacts, a TE correction is performed by dividing the signal intensity of each pixel by either  $\exp(-\Delta TE/T_2^*)$  or  $\exp(-\Delta TE/T_2)$  depending on the sign of  $\Delta k_y$  (Fig. 1E), where  $1/T_2^* = 1/T_2 + 1/T_2'$  and  $1/T_2' = 1/T_2 - 1/T_2'$  (3).  $\Delta TE$  is computed as  $|\Delta k_y| T_{ESP}$ , where  $\Delta k_y$  is obtained from the  $\Delta k_y$  map and  $T_{ESP}$  is the echo spacing of the EPI readout.

Three DTI scans of a healthy volunteer were performed on a 3 T GE scanner using 28 overscans (TE = 103 ms), 12 overscans (TE = 73 ms), and 12 overscans with blips, as well as TR = 4 s, matrix size =  $96 \times 96$ , voxel size =  $(2.5 \text{ mm})^3$ , 20 slices,  $b = 1000 \text{ s/mm}^2$ , 15 diffusion directions, and  $T_{ESP} = 944 \mu\text{s}$ . The phantom DTI scan was performed using 28 overscans. The TE correction assumed that  $T_2/T_2^* = 80/47 \text{ ms}$  for white matter (4).

## Results and Discussion

The phantom  $\Delta k_y$  maps show that  $\Delta k_y$  varies significantly with the diffusion direction and slice number (Fig. 2). The variation is larger for odd slices, which were acquired first in this interleaved acquisition, and decreases for even slices, when long time constant ( $> 200 \text{ ms}$ ) eddy currents extending over multiple slice acquisitions reach a steady-state.

Representative *in vivo* results are shown in Figs. 3–5 for two diffusion directions. With 28 overscans, the echoes are shifted from the  $k_y = 0$  line (Fig. 3A, dashed line), but remain within the acquired k-space, and the reconstructed images have a low SNR because of the long TE (Fig. 4A). With 12 overscans, the echoes are shifted outside the acquired k-space (Fig. 3B), resulting in severe type 1 artifacts (Fig. 4B, arrows). By adding appropriate blips, the echoes are shifted back to the  $k_y = 0$  line (Fig. 3C) and the signal loss is recovered, but type 2 artifacts remain (Fig. 4C, arrows). By using the multischeme PF reconstruction, both types of artifact are effectively corrected for and the SNR is increased by  $\sim 30\%$  because of the shorter TE (Fig. 4D). The  $\Delta k_y$  maps show that for 28 overscans, regions with  $\Delta k_y \gg 0$  (Fig. 5A, arrows) correspond to type 1 artifacts, whereas for 12 overscans with blips, regions with  $\Delta k_y \ll 0$  (Fig. 5B, arrows) correspond to type 2 artifacts, as expected.

With 28 overscans, the FA map has a low SNR (Fig. 6A). With 12 overscans, type 1 artifacts lead to substantial FA errors (Fig. 6B, arrow). By using blips and multischeme PF reconstruction, type 1 and 2 artifacts are corrected for, but type 3 artifacts still result in significant FA errors (Fig. 6C, arrows), as  $\Delta TE$  can reach up to 30 ms. After TE correction, all three types of artifact are corrected for (Fig. 6D).

These results demonstrate that the proposed PF-DTI acquisition and post-processing method can effectively correct for all three types of artifact caused by eddy current-induced echo shifts while maintaining a high SNR.

## References

(1) Chen NeuroImage 2006;31:609 (2) Chen MRM 2008;59:916 (3) Yablonskiy MRM 1997;37:872 (4) Wansapura JMRI 1999;9:531. Support: NIH grants NS41328 and NS65344.

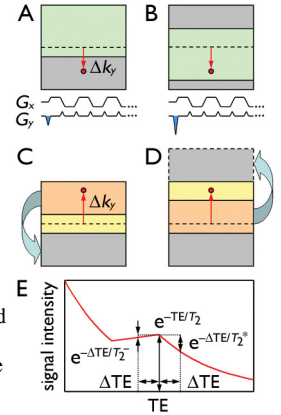


Fig. 1: Type 1 (A), 2 (C), and 3 (E) artifacts. Blipped DTI acquisition (B). Multischeme PF reconstruction (D).

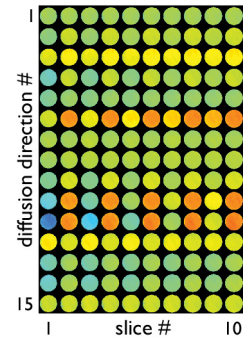


Fig. 2:  $\Delta k_y$  maps for 15 diffusion directions and the first 10 slices (out of 20).

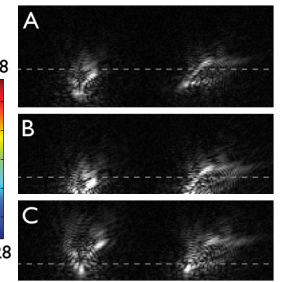


Fig. 3: k-space data for two diffusion directions (6 & 12) and 28 overscans (A), 12 overscans (B), and 12 overscans with blips (C).

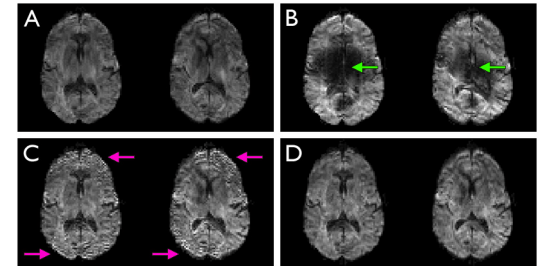


Fig. 4: DTI images for 28 overscans (A), 12 overscans (B), 12 overscans with blips (C), and 12 overscans with blips and multischeme PF reconstruction (D). Same scaling.

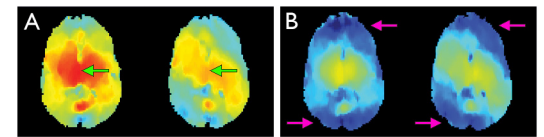


Fig. 5:  $\Delta k_y$  maps for 28 overscans (A) and 12 overscans with blips (B). Same scaling as in Fig. 1.

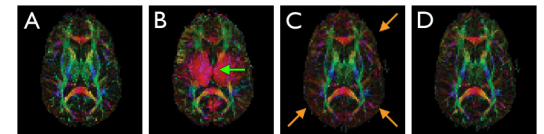


Fig. 6: Color-coded FA maps for 28 overscans (A), 12 overscans (B), 12 overscans with blips and multischeme PF reconstruction (C), and 12 overscans with blips, multischeme PF reconstruction, and TE correction (D).